| | |
|---|---|
| **Preprint Title** | Approaching microwave photon sensitivity with Al Josephson junction |
| **Authors** | Andrey L. Pankratov, Anna V. Gordeeva, Leonid S. Revin, Dmitry A. Ladeynov, Anton A. Yablokov and Leonid S. Kuzmin |
| **Publication Date** | 30 März 2022 |
| **Article Type** | Full Research Paper |
| **ORCID® iDs** | Andrey L. Pankratov - https://orcid.org/0000-0003-2661-2745; Anna V. Gordeeva - https://orcid.org/0000-0001-6948-3950; Leonid S. Revin - https://orcid.org/0000-0003-1645-4122; Dmitry A. Ladeynov - https://orcid.org/0000-0001-6856-7079 |

# Approaching microwave photon sensitivity with Al Josephson junction

A. L. Pankratov[1,2,3], A. V. Gordeeva*[1,2], L. S. Revin[1,2], D. A. Ladeynov[1,2,3], A. A. Yablokov[1,2] and L. S. Kuzmin[1,4, 1, 2, 3, 4]

Address: [1]Nizhny Novgorod State Technical University n.a. R.E. Alekseev, GSP-41, Nizhny Novgorod, 603950, Russia; [2]Institute for Physics of Microstructures of RAS, GSP-105, Nizhny Novgorod, 603950, Russia; [3]Lobachevsky State University of Nizhny Novgorod, 603950, Nizhny Novgorod, Russia and [4]Chalmers University of Technology, 41296, Gothenburg, Sweden

Email: A. V. Gordeeva - a.gordeeva@nntu.ru

* Corresponding author

## Abstract

Here we experimentally test the applicability of aluminum Josephson junction of few microns size as a single photon counter in microwave frequency range. We have measured the switching from the superconducting to the resistive state due to absorption of 10 GHz signal. The dependence of the switching probability on the signal power suggests that the switching is initiated by simultaneous absorption of three and more photons with the dark count time above 0.01 s.

## Keywords

Josephson junction, microwave photons, single photon counter, thermal activation

# Introduction

The development of a single photon counter (SPC) for tenths of GHz is demanded by several application fields, at least for the last two decades. The difficulty of this development is in the small energy scale: the energy of a photon of 10 GHz is just 7 yoctojoule ($7 \cdot 10^{-24}$ J). To realize the detection, the photon must trigger a process, whose energy is of the order of this value (the difference between initial and excited states). There are not many examples in solid-state physics with such energy scales. Moreover, another difficulty is that the spontaneous change of the state must be significantly less probable so that the detector could be in a waiting mode for a significant amount of time.

The superconductor-insulator-superconductor (SIS) junctions have not previously been seriously considered for the role of detectors of single photons in the microwave range, despite the sporadic works showing such a possibility [1-7]. Recently, the interest to microwave SPC has been increased [8,9] due to new experiments of dark matter search [10-12] and the corresponding program, initiated by INFN in Italy [13-17].

Our experiments show that typical aluminium Josephson junctions can indeed have a few-photon sensitivity in microwave frequency range, and a photon counter can be made on their basis. We use the metastable quasi-equilibrium state of a Josephson junction (JJ), which at low temperatures is stable enough for thermal fluctuations and quantum tunneling, but can be easily destroyed by absorption of a single photon. We demonstrate few-photon sensitivity of our samples in a single-shot regime and outline the junction parameter range, where approaching of single photon sensitivity is possible.

# Results and Discussion

In this section we describe our experimental setup, as well as the measurement results and comparison with theory.

To study the dynamic of a SIS tunnel junction, we have thermally anchored the sample to the mixing chamber of a He3/He4 dilution refrigerator Triton 200 from Oxford Instruments. A block diagram of the experimental setup, including filtering and room temperature electronics, is shown in Fig. 1a. The sample (Fig. 1b) was mounted in an RF-tight box with a superconducting shielding on the coldest plate. The dc-bias wires were filtered with feed-through capacitors at room temperature and RC filters at the 10 mK cryostat plate, minimizing the effect of unwanted low-frequency noise.

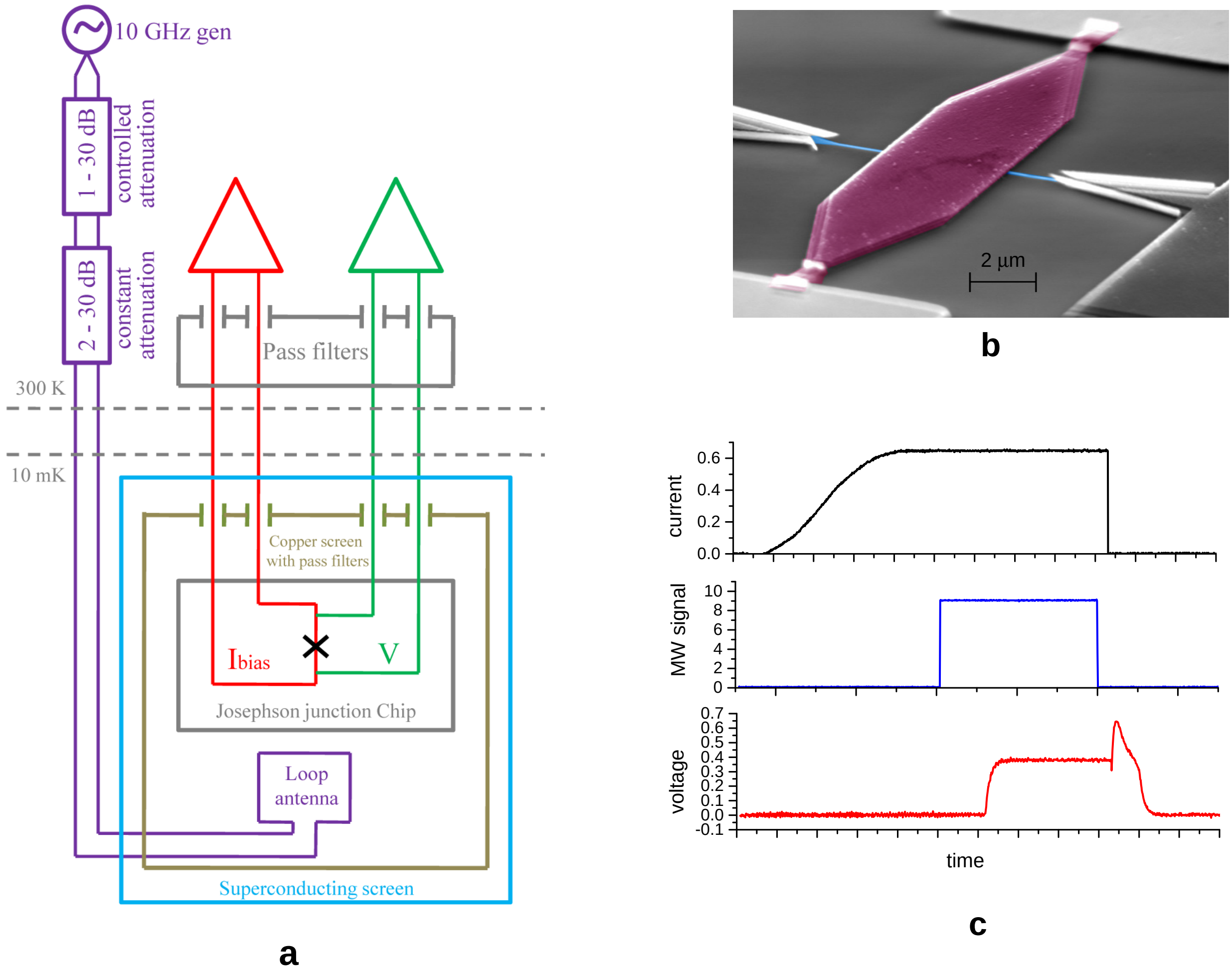


**Figure 1:** (a) The scheme of measurement electronics with thermal anchoring and various filtering stages. (b) The SEM image of the SIS junction. The top electrode is highlighted by magenta colour, the bottom electrode (blue colour) has the same shape as the top one in the area of the tunnel barrier. (c) The time diagram of the channels: current through the JJ, amplitude of the microwave signal and voltage across the JJ.

For a high-frequency experiment, a microwave signal was fed into the cryostat via a phosphor bronze twisted-pairs with attenuation of -15 dB per meter at 10 GHz and with a loop antenna near the JJ. The RF signal from the external microwave synthesizer was attenuated using constant attenuators from 2 dB to 30 dB and voltage controlled room-temperature attenuator, preliminarily calibrated with a commercial spectrum analyzer. The high-frequency signal was varied from a high power at which the photon assisted tunneling steps are well pronounced at the IV-curve [18], to a low power whose presence can be observed only in the switching probabilities and in the decrease of the superconducting state lifetime.

The time traces of setting a current and an external microwave signal to measure the switching probability as a function of power are shown in Fig. 1c. First, the current through the junction is increased up to the required value by $\sin^2$ law [19] to realize a quasi-adiabatic ramping, then the microwave signal is turned on for a fixed time slot. Due to strong attenuation of harmonic signal, the microwave pulse represents sequence of single photons, pairs, triples and so on, which obey Poisson distribution [20,21]. After turning off the signal, the state of the JJ is checked. Depending on whether the JJ is in the resistive or superconducting state, the unity or zero is added to the switching probability, respectively.

We begin our consideration of the Josephson junction as a photon counter with its current-voltage characteristic (see Fig. 2a) and the determination of the critical current. All further analysis of experimental results and understanding of the energy relations of the JJ in comparison with the energy of photons (see Fig. 2b) depends on the accuracy of determining the critical current. The Al Josephson junction with the area $60\mu m^2$ and with the critical current $I_c \approx 8.6\ \mu$A has been measured, see the SEM image of the sample in Fig. 1b. Due to rather low noise measuring environment, used before for THz receiver applications [22,23], one can see in Fig. 2a a typical current-voltage characteristics (IVC) with the critical current, close to a theoretical value [24]. Besides, a subgap structure is visible at the inverse branch of the IVC. Such a structure with peculiarities in the differential resistance at voltages $2\delta/n$ was calculated theoretically for normal metal links between two superconductors as multiple Andreev reflections [25] and observed in experiment both for SNS and SIS junctions [26].

In difference with smaller junctions [7], where the phase-diffusion regime is possible [27-32], the analyzed junction demonstrates a typical behavior [4,33], i.e. a monotonic increase of the switching current distribution width with the rise of the temperature, see Fig. 3. For the switching current measurements, the bias current of the junction was ramped up at a constant rate. The voltage was measured using a low noise room-temperature differential amplifier AD745 and was fed to a high-

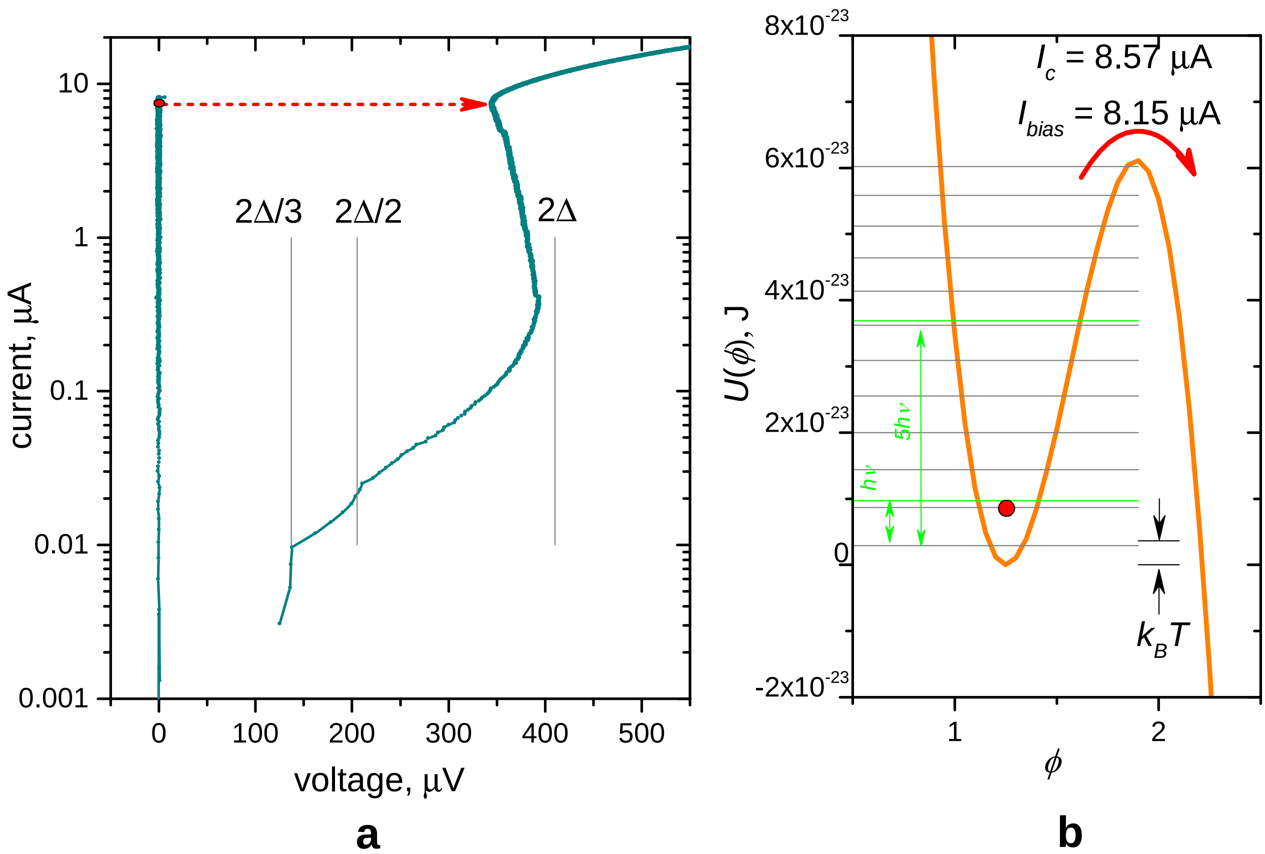


**Figure 2:** (a) The current-voltage characteristics of the Josephson junction with $I_c = 8.6$ $\mu$A at 50 mK. The red point indicates the state of JJ in a "waiting" mode, the arrow shows a jump to the resistive state after absorption of photons. (b) The potential profile at the bias current 8.15 $\mu$A. Energy of 1 and 5 photons are shown by lines relative to the minimum energy level. Under these conditions, the JJ switches with probability 1 if 5 photons are absorbed simultaneously (q[5] = 1), and with probability 0.13 if 4 photons are absorbed (q[4]=0.13). These probabilities are obtained from the fitting of experimental data, see Fig. 5 below. The scale of the effective thermal fluctuation energy is given by black arrows for $T = 265mK$ (see the main text).

speed NI ADC card. The switching current histograms were collected in the temperature range between 1 K and 30 mK. The dependence of their width on temperature is shown in Fig. 3. It is interesting to note the crossover temperature to the quantum regime of about 250 mK, which is somewhat lower than in [33] for junctions with larger critical currents.

As known, the switching current to the resistive state depends on the sweep rate, therefore, its value is underestimated in dc measurements. The upper limit is given by the BCS expression $1.75kT_c/(eR_N)$ [24], which depends on the critical temperature of the electrodes and the normal resistance of the tunnel barrier only. This maximum possible critical current is difficult to achieve

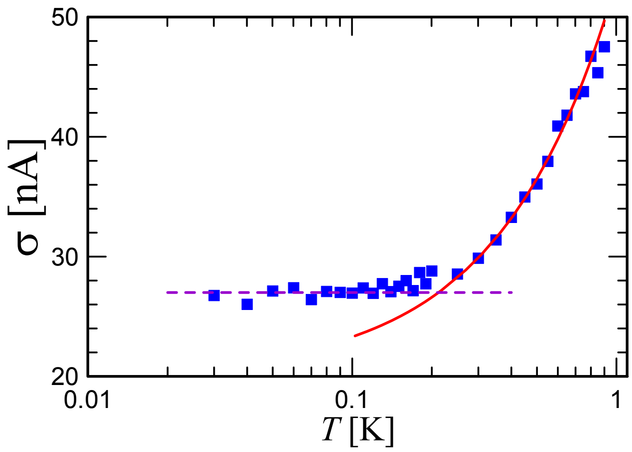


**Figure 3:** The width of the switching current distribution of the Josephson junction. One can see a standard behavior when the distribution width grows monotonically with increase of the temperature. Here the violet dashed line shows the quantum regime and the red solid curve shows the thermal activation regime.

in real junctions. In our opinion, the most reliable way to determine the critical current is to compare the experimental lifetime as a function of the current with the lifetime calculated using numerical simulations [34,35] in the frame of the resistively-capacitively shunted junction (RCSJ) model [24]. It is important to use the RCSJ model in the temperature range where it is valid, i.e. above the crossover temperature in the quantum regime.

The lifetime (dark count time) measurements are organized as follows. The current through the junction is quasi-adiabatically ramped up to a given value. After reaching the required bias current, the countdown of lifetimes begins until the moment of jumping to the resistive branch. This cycle is repeated 100 - 200 times to collect statistics, after which the average value of the switching time and its standard deviation are calculated.

Since the considered Josephson junction is standard and there is no phase diffusion regime observed (see Fig. 3), there is no mixed mode of operation, where a part of the time there are short voltage pulse due to escapes to the adjacent potential minima, and a part of the time the voltage is zero. This makes it easier to determine the lifetime in the numerical model. In this case, the JJ is considered to be switched if the phase exceeds a certain threshold value, usually chosen to the right of the position of the nearest maximum of the potential for a given bias current.

The need to use numerical simulation is due to the fact that in the experiment we are limited by the

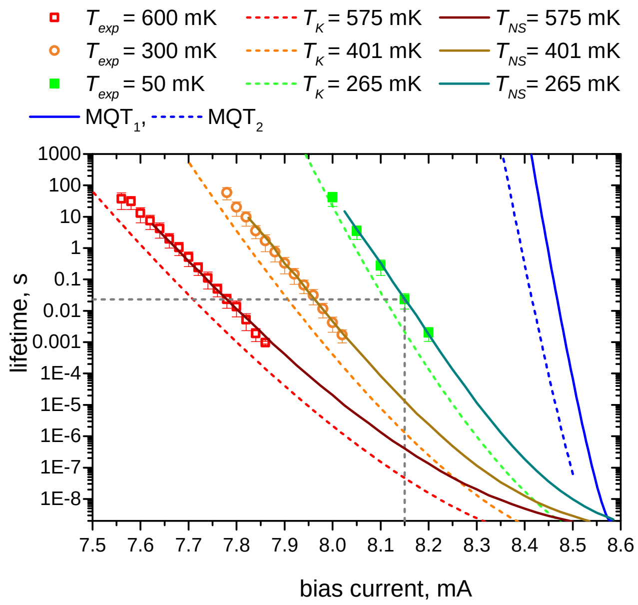


**Figure 4:** The lifetime the junction versus bias current at temperatures 50 mK (green), 300 mK (orange), 600 mK (red). Here fitting is performed using the approximate Kramers' formula (1) (dashed curve) and using the numerical solution of the Langevin equation with noise (solid curve). In the latter case the agreement is rather good.

time constant of the filters that provide suppression of external interferences. As a result we cannot measure switching times faster than the time constant, which in our case is about 1 ms. To obtain shorter times, we numerically solve the Langevin equation with noise source [34,35] in the frame of RCSJ model, which has been proven for classical JJs in the thermal regime [24]. Its applicability is also confirmed for our case by a good overlap with the experimental data.

It is seen from Fig. 4 that the experimental points at 300 and 600 mK agree well with the simulation results if the parameters for numerical calculations are 401 mK, Ic = 8.536 $\mu A$ and 575 mK, Ic = 8.51 $\mu A$, respectively. It is interesting to note that even the curve for 50 mK is well fitted if the critical current is set to 8.586 $\mu A$ and the temperature is 265 mK, which is close to the crossover temperature, deduced from Fig. 3. For the same parameters, the lifetime was calculated with a well-known Kramers' formula [36-41], modified for intermediate damping values [42,43]:

$$\tau = \frac{a_t \exp{(\Delta u/\gamma)}}{(1-i^2)^{1/4}}, \quad a_t = 4\left(\sqrt{1+\frac{\alpha\gamma}{3.6\sqrt{1-i^2}}}+1\right)^{-2} \tag{1}$$

The used notations are: $i = I_{bias}/I_C$ is the dimensionless bias current with the bias current $I_{bias}$

and the critical current $I_C$, $\Delta u = 2\sqrt{1-i^2} + 2i(\arcsin(i) - \pi/2)$ is the potential barrier height, $\gamma = I_T/I_C$ is the noise intensity, and $I_T = 2ekT/\hbar$ is the fluctuational current which can be calculated as: $I_T[\mu\text{A}] = 0.042T[\text{K}]$ [24] for a given temperature $T$. Note that, the thermal current is 2.1 nA for 50 mK and 21 nA for 500 mK, respectively. The investigated junction also demonstrates a typical Kramers' dependence of the lifetime, see Fig. 4, but the analytical estimates (1) give an underestimated lifetime compared to a more accurate numerical calculation.

Thus, the critical current at a temperature of 50 mK was determined as 8.586 $\mu A$. For this $I_c$ value, the tunneling time versus the bias current was calculated, which is believed to be the reason that below the crossover temperature, the lifetime stops changing. The results are shown as a solid blue curve if the tunneling occurs from the minimum of the potential profile [43], and as a dotted blue curve – if from the zero energy level [44]. As can be seen, these curves have a steeper slope than the experimental lifetime at 50 mK. This may indicate that we do not reach the true quantum regime, and the lifetime stops changing with decreasing temperature due to either residual low frequency interference or overheating. Additional experiments are planned to determine this issue.

The absorption of a photon increases the energy of a JJ by a certain value and may result in switching into the resistive state. There are several frequency ranges of effective detection may exist [34] due to resonant activation and the most efficient switching occurs at signal frequencies of 0.6 from $\omega_p = (2eI_c/\hbar C)^{1/2}$ [35], which is fully consistent with the parameters of the considered experiment. In the current work we measure the probability of switching initiated by 10 GHz signal with a fixed duration $t_{pulse} = 0.05$ s. The plasma frequency of the junction is 15.6 GHz, while at the bias current of 815 μA, where we presumably see three-photon sensitivity, the resonant frequency $\omega_r$ of the Josephson junction oscillation circuit $\omega_r = \omega_p(1-i^2)^{1/4}$ is 8.8 GHz.

The statistics of switching versus an absorbed power is illustrated in Fig. 5a,b for several bias currents and temperatures 50 and 500 mK, respectively. Each curve in Fig. 5 has been collected with $(200 - 10^4)$ averages of switching events.

The experimental results in Fig. 5a,b can be reproduced using the Poissonian distribution of photons [18]:

$$p_{sw} = 1 - (1 - p_{\delta t})^M \,,$$
$$p_{\delta t} = e^{-N}\left(q[0] + q[1]N + q[2]\frac{N^2}{2!} + q[3]\frac{N^3}{3!} + \ldots\right), \tag{2}$$

where $M$ is the number of attempts, $q[0]$ is the probability of the erroneous detection without a photon, and $q[1]$, $q[2]$, $q[3]$ are the detection efficiencies of 1, 2, 3, etc., photons. The slope of the fitting curves is set by the number of photons, triggering the switching. The position on the power axis is determined by the effective system response time $dt$ and by the efficiency of switching $q$. The fitting curves in Fig. 5a are obtained with $dt = 0.3$ ns for slope 3 and $dt = 5.7$ ns for slope 15. The curve with slope 3 fits the experimental data for the bias current 8.15 $\mu$A quite well if q-array is $[5\cdot10^{-10},\ 5\cdot10^{-10},\ 5\cdot10^{-10},\ 0.002,\ 0.13,\ 1,\ 1,\ ...]$. Therefore, the probability to switching due to the absorption of 3 photons is 0.002. In Fig. 2b the barrier height is compared with the energy of one photon. The potential profile is calculated for the critical current 8.586 $\mu$A. The photon frequency and energy are 10 GHz and $6.8 \cdot 10^{-24}$ J. The energy of 3 and even 5 photons are less than the barrier height. However, the switching may still happen due to either resonant tunnelling or resonant activation effects [17,34,35,43,45].

With the critical current 8.586 $\mu$A, the barrier height for bias currents in the range $(7.5 - 8.08)$ $\mu$A equals to the energy of $(35-11)$ photons. This number is quite close to the number we get from the fitting of probability versus power slopes: $(15 - 3)$. Even if the total energy of absorbed photons is less than the barrier height, the probability to switch to the resistive state by tunneling increases significantly.

In Fig. 5 one can see how the switching probability evolves with increasing temperature from 50 mK to 500 mK. The difference is not very large because at 50 mK the effective temperature was rather 265 mK, according to numerical simulations, and the thermal current at 500 mK is much smaller than the critical current. There is still 3-photon sensitivity with efficiency 0.01 but for a slightly lower bias current $8\mu A$. Curves for other bias currents can be fitted with slopes 4, 5, 6, 9 and 12.

The small difference between results at 50 mK (265 mK) and 500 mK can be understood from Fig. 2b. The superconducting gap decreases by a few percent due to temperature increase from 265 to 500 mK according to BCS model. It leads to the minor decrease of the JJ critical current. Thus, the qualitative picture remains the same for 265 and 500 mK: the height of the potential barrier is still several times larger than the thermal energy and the energy of single 10 GHz photons.

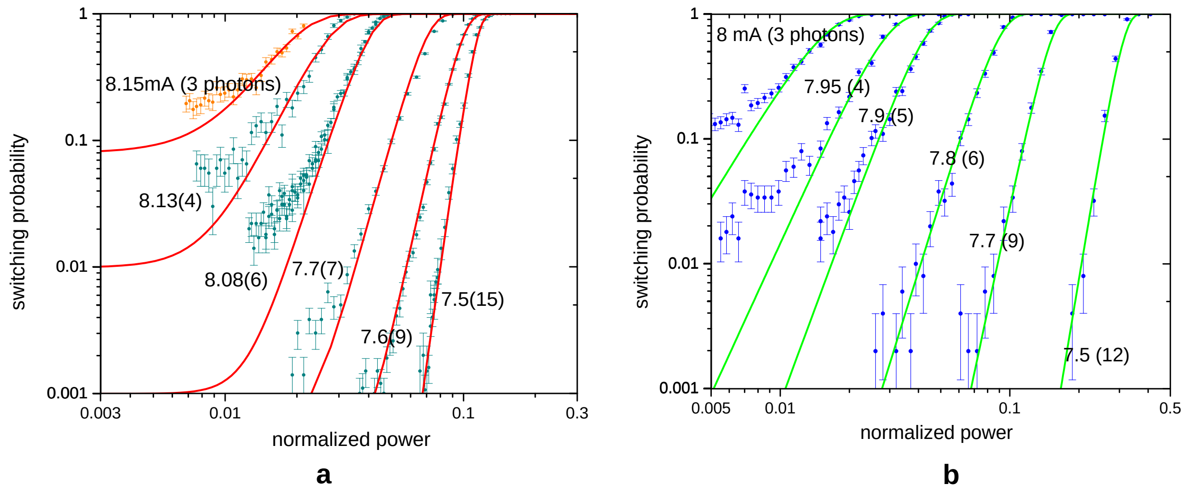


**Figure 5:** The switching probability of JJ versus power of the signal (with duration 50 ms) for different bias currents. The dots with error bars are experimental data. For each switching event, the system was first prepared in the initial state by quasi-adiabatically ramping the bias current during 0.05 s. If the microwave signal caused a switching to the finite voltage state during the driving pulse, such event was counted as 1, and 0 otherwise. (a) T = 50 mK. The orange dots are for the bias 8.15 $\mu$A. The red fitting curves are obtained with formula (2). (b) T = 500 mK. The green fitting curves are obtained with formula (2).

# Conclusions

We have presented an experimental study of a Josephson junction with the area 60 $\mu m^2$ and the critical current 8.6 $\mu A$ for application as a single photon counter in microwave frequency range. Using a strongly attenuated 10 GHz harmonic signal with Poisson distribution of photons as the photon source, three-photon sensitivity with efficiency 0.002 and the dark count time 0.02 s has been shown.

From the analysis of the lifetime we see that there is a room for improvement of the sensitivity if residual low frequency noise or overheating of the junction could be decreased. The source of the issue and the way of its suppression need to be investigated in further experiments.

Comparing the obtained results for the considered sample and small area junctions [7,18], we can conclude that the optimal critical current range, allowing improving both sensitivity and dark count time, lie in the area of hundreds nA critical current junctions as predicted in [6]. Such junctions are now currently being measured.

**Table 1:** Parameters of the JJ.

| **parameter** | **experiment** | **fit** |
|---|---|---|
| $I_c$ [nA] | 8160 | 8586 |
| $R_N$ [Ω] | 29 | 29 |
| $C$ [fF] | 2700 | 2700 |
| Area [$\mu$m$^2$] | 60 | – |

## Acknowledgements

The samples were fabricated in the Chalmers Nanotechnology Centre. The measurements were performed using the facilities of the Laboratory of Superconducting Nanoelectronics of NNSTU. The SEM image of the sample was obtained using the Common Research Centre “Physics and technology of micro- and nanostructures” of IPM RAS.

## Funding

The work is supported by the Russian Science Foundation (Project No. 19-79-10170).

# References

1. Wallraff, A.; Duty, T.; Lukashenko, A.; Ustinov, A. V. *Physical Review Letters* **2003**, *90* (3), 037003. doi:10.1103/PhysRevLett.90.037003.

2. Chen, Y.-F.; Hover, D.; Sendelbach, S.; Maurer, L.; Merkel, S. T.; Pritchett, E. J.; Wilhelm, F. K.; McDermott, R. *Physical Review Letters* **2011**, *107* (21), 217401. doi:10.1103/PhysRevLett.107.217401.

3. Poudel, A.; McDermott, R.; Vavilov, M. G. *Physical Review B* **2012**, *86* (17), 174506. doi: 10.1103/PhysRevB.86.174506.

4. Oelsner, G.; Revin, L. S.; Il'ichev, E.; Pankratov, A. L.; Meyer, H.-G.; Grönberg, L.; Hassel, J.; Kuzmin, L. S. *Applied Physics Letters* **2013**, *103* (14), 142605. doi:10.1063/1.4824308.

5. Oelsner, G.; Andersen, C. K.; Rehák, M.; Schmelz, M.; Anders, S.; Grajcar, M.; Hübner, U.; Mølmer, K.; Il'ichev, E. *Physical Review Applied* **2017**, *7* (1), 014012. doi:10.1103/PhysRevApplied.7.014012.

6. Kuzmin, L. S.; Sobolev, A. S.; Gatti, C.; Di Gioacchino, D.; Crescini, N.; Gordeeva, A.; Il'ichev, E. *IEEE Transactions on Applied Superconductivity* **2018**, *28* (7), 2400505. doi:10.1109/TASC.2018.2850019.

7. Revin, L. S.; Pankratov, A. L.; Gordeeva, A. V.; Yablokov, A. A.; Rakut, I. V.; Zbrozhek, V. O.; Kuzmin, L. S. *Beilstein Journal of Nanotechnology* **2020**, *11* (1), 960–965. doi:10.3762/bjnano.11.80.

8. Kokkoniemi, R.; Girard, J.-P.; Hazra, D.; Laitinen, A.; Govenius, J.; Lake, R. E.; Sallinen, I.; Vesterinen, V.; Partanen, M.; Tan, J. Y.; Chan, K. W.; Tan, K. Y.; Hakonen, P.; Möttönen, M. *Nature* **2020**, *586* (7827), 47–51. doi:10.1038/s41586-020-2753-3.

9. Lee, G.-H.; Efetov, D. K.; Jung, W.; Ranzani, L.; Walsh, E. D.; Ohki, T. A.; Taniguchi, T.; Watanabe, K.; Kim, P.; Englund, D.; Fong, K. C. *Nature* **2020**, *586* (7827), 42–46. doi:10.1038/s41586-020-2752-4.

10. Barbieri, R.; Braggio, C.; Carugno, G.; Gallo, C. S.; Lombardi, A.; Ortolan, A.; Pengo, R.; Ruoso, G.; Speake, C. C. *Physics of the Dark Universe* **2017**, *15*, 135–141. doi:10.1016/j.dark.2017.01.003.

11. Crescini, N.; Alesini, D.; Braggio, C.; Carugno, G.; D'Agostino, D.; Di Gioacchino, D.; Falferi, P.; Gambardella, U.; Gatti, C.; Iannone, G.; Ligi, C.; Lombardi, A.; Ortolan, A.;

Pengo, R.; Ruoso, G.; Taffarello, L. *Physical Review Letters* **2020**, *124* (17), 171801. doi: 10.1103/PhysRevLett.124.171801.

12. McAllister, B. T.; Flower, G.; Ivanov, E. N.; Goryachev, M.; Bourhill, J.; Tobar, M. E. *Physics of the Dark Universe* **2017**, *18*, 67–72. doi:10.1016/j.dark.2017.09.010.

13. Alesini, D.; Babusci, D.; Barone, C.; Buonomo, B.; Beretta, M. M.; Bianchini, L.; Castellano, G.; Chiarello, F.; Di Gioacchino, D.; Falferi, P.; Felici, G.; Filatrella, G.; Foggetta, L. G.; Gallo, A.; Gatti, C.; Giazotto, F.; Lamanna, G.; Ligabue, F.; Ligato, N.; Ligi, C.; Maccarrone, G.; Margesin, B.; Mattioli, F.; Monticone, E.; Oberto, L.; Pagano, S.; Paolucci, F.; Rajteri, M.; Rettaroli, A.; Rolandi, L.; Spagnolo, P.; Toncelli, A.; Torrioli, G. *Journal of Low Temperature Physics* **2020**, *199* (1), 348–354. doi:10.1007/s10909-020-02381-x.

14. Alesini, D.; Babusci, D.; Barone, C.; Buonomo, B.; Beretta, M. M.; Bianchini, L.; Castellano, G.; Chiarello, F.; Di Gioacchino, D.; Falferi, P.; Felici, G.; Filatrella, G.; Foggetta, L. G.; Gallo, A.; Gatti, C.; Giazotto, F.; Lamanna, G.; Ligabue, F.; Ligato, N.; Ligi, C.; Maccarrone, G.; Margesin, B.; Mattioli, F.; Monticone, E.; Oberto, L.; Pagano, S.; Paolucci, F.; Rajteri, M.; Rettaroli, A.; Rolandi, L.; Spagnolo, P.; Toncelli, A.; Torrioli, G. *Journal of Physics: Conference Series* **2020**, *1559* (1), 012020. doi:10.1088/1742-6596/1559/1/012020.

15. Pountougnigni, O. V.; Yamapi, R.; Tchawoua, C.; Pierro, V.; Filatrella, G. *Physical Review E* **2020**, *101* (5), 052205. doi:10.1103/PhysRevE.101.052205.

16. Piedjou Komnang, A. S.; Guarcello, C.; Barone, C.; Gatti, C.; Pagano, S.; Pierro, V.; Rettaroli, A.; Filatrella, G. *Chaos, Solitons & Fractals* **2021**, *142*, 110496. doi:10.1016/j.chaos.2020.110496.

17. Chiarello, F.; Alesini, D.; Babusci, D.; C., B.; Beretta, M. M.; Buonomo, B.; et al., *IEEE Transactions on Applied Superconductivity* **2022**, *32* (4), 1100305. doi:10.1109/TASC.2022.3148693.

18. Pankratov, A. L.; Revin, L. S.; Gordeeva, A. V.; A., Y. A.; Kuzmin, L. S.; V., I. E. *npj Quantum Information* **2022**, under consideration.

19. Revin, L. S.; Pankratov, A. L. *Applied Physics Letters* **2011**, *98* (16), 162501. doi:10.1063/1.3582615.

20. Gol'tsman, G. N.; Okunev, O.; Chulkova, G.; Lipatov, A.; Semenov, A.; Smirnov, K.; Voronov, B.; Dzardanov, A.; Williams, C.; Sobolewski, R. *Applied Physics Letters* **2001**, *79* (6), 705–707. doi:10.1063/1.1388868.

21. Fox, M. *Quantum Optics: An Introduction*; Oxford University Press, 2006; Vol. 15.

22. Gordeeva, A. V.; O., Z. V.; Pankratov, A. L.; Revin, L. S.; Shamporov, V. A.; Gunbina, A. A.; Kuzmin, L. S. *Applied Physics Letters* **2017**, *110* (16), 162603. doi:10.1063/1.4982031.

23. Kuzmin, L. S.; Pankratov, A. L.; Gordeeva, A. V.; Zbrozhek, V. O.; Shamporov, V. A.; Revin, L. S.; Blagodatkin, A. V.; Masi, S.; de Bernardis, P. *Communications Physics* **2019**, *2* (104), 1–8. doi:10.1038/s42005-019-0206-9.

24. Likharev, K. K. *Dynamics of Josephson junctions and circuits*; Gordon and Breach Science Publishers: New York, 1986.

25. Klapwijk, T.; Blonder, T.; M., T. *Physica B+C* **1982**, *109-110*, 1657–1664. doi:https://doi.org/10.1016/0378-4363(82)90189-9. 16th International Conference on Low Temperature Physics, Part 3

26. Kleinsasser, A.; Miller, R.; Mallison, W.; Arnold, G. *Physical review letters* **1994**, *72* (11), 1738–1741. doi:10.1103/PhysRevLett.72.1738.

27. Martinis, J. M.; Kautz, R. L. *Physical Review Letters* **1989**, *63* (14), 1507–1510. doi:10.1103/PhysRevLett.63.1507.

28. Vion, D.; Götz, M.; Joyez, P.; Esteve, D.; Devoret, M. H. *Physical Review Letters* **1996**, *77* (16), 3435–3438. doi:10.1103/PhysRevLett.77.3435.

29. Kivioja, J. M.; Nieminen, T. E.; Claudon, J.; Buisson, O.; Hekking, F. W. J.; Pekola, J. P. *Physical Review Letters* **2005**, *94* (24), 247002. doi:10.1103/PhysRevLett.94.247002.

30. Koval, Y.; Fistul, M. V.; Ustinov, A. V. *Physical Review Letters* **2004**, *93* (8), 087004. doi:10.1103/PhysRevLett.93.087004.

31. Longobardi, L.; Massarotti, D.; Stornaiuolo, D.; Galletti, L.; Rotoli, G.; Lombardi, F.; Tafuri, F. *Physical Review Letters* **2012**, *109* (5), 050601. doi:10.1103/PhysRevLett.109.050601.

32. Lisitskiy, M.; Massarotti, D.; Galletti, L.; Longobardi, L.; Rotoli, G.; Russo, M.; Tafuri, F.; Ruggiero, B. *Journal of Applied Physics* **2014**, *116* (4), 043905. doi:10.1063/1.4890317.

33. Wallraff, A.; Lukashenko, A.; Duty, T.; Coqui, C.; Kemp, A.; Ustinov, A. V. *Review of Scientific Instruments* **2003**, *74* (8), 3740. doi:DOI:10.1063/1.1588752.

34. Yablokov, A. A.; Mylnikov, V. M.; Pankratov, A. L.; Pankratova, E. V.; Gordeeva, A. V. *Chaos, Solitons & Fractals* **2020**, *136*, 109817. doi:10.1016/j.chaos.2020.109817.

35. Yablokov, A. A.; Glushkov, E. I.; Pankratov, A. L.; Gordeeva, A. V.; Kuzmin, L. S.; Il'ichev, E. V. *Chaos, Solitons & Fractals* **2021**, *148*, 111058. doi:10.1016/j.chaos.2021.111058.

36. Kramers, H. A. *Physica* **1940**, *7* (4), 284–304. doi:10.1016/S0031-8914(40)90098-2.

37. Hänggi, P.; Talkner, P.; Borkovec, M. *Reviews of Modern Physics* **1990**, *62* (2), 251–341. doi:10.1103/RevModPhys.62.251.

38. Malakhov, A.; Pankratov, A. *Physica A* **1996**, *29* (1), 109–126. doi:10.1016/0378-4371(95)00395-9.

39. Malakhov, A. N.; Pankratov, A. L. *Physica C: Superconductivity* **1996**, *269* (1), 46–54. doi:10.1016/0921-4534(96)00426-1.

40. Malakhov, A. *Chaos* **1997**, *7* (06), 488. doi:10.1063/1.166220.

41. Blackburn, J. A.; Cirillo, M.; Grønbech-Jensen, N. *Physics Reports* **2016**, *611*, 1–33. doi:10.1016/j.physrep.2015.10.010.

42. Büttiker, M.; Harris, E. P.; Landauer, R. *Phys. Rev. B* **1983**, *28*, 1268–1275. doi:10.1103/PhysRevB.28.1268.

43. Martinis, J. M.; Devoret, M. H.; Clarke, J. *Physical Review B* **1987**, *35* (10), 4682–4698. doi:10.1103/PhysRevB.35.4682.

44. Golubev, D. S.; Il'ichev, E. V.; Kuzmin, L. S. *Physical Review Applied* **2021**, *16* (1), 014025. doi:10.1103/PhysRevApplied.16.014025.

45. Devoret, M. H.; Martinis, J. M.; Esteve, D.; Clarke, J. *Physical Review Letters* **1984**, *53* (13), 1260–1263. doi:10.1103/PhysRevLett.53.1260.